

Effect of cooling rate on the solidification characteristics and dendrite coherency point of ADC12 aluminum die casting alloy using thermal analysis

M. Malekan¹ · S. Naghdali² · S. Abrishami² · S. H. Mirghaderi²

Received: 9 August 2015 / Accepted: 28 December 2015
© Akadémiai Kiadó, Budapest, Hungary 2016

Abstract In the metal casting industry, an improvement of component quality depends mainly on better control over the production parameters. Thus, computer-aided cooling curve thermal analysis is a very useful method for easy and fast evaluation of a variety of properties. In this work, the effect of different cooling rates ($1.2\text{--}7.2\text{ }^\circ\text{C s}^{-1}$) on solidification parameters and dendrite coherency point (DCP) of ADC12 aluminum alloy was investigated by thermal analysis. The results revealed that solidification parameters and dendrite coherency point are influenced by variation of cooling rate. Increasing the cooling rate can increase the temperature interval of coherency ($T_N\text{--}T_{\text{DCP}}$) and coherency fraction solid (f_s^{DCP}) about $31\text{ }^\circ\text{C}$ and 11% , respectively, but the coherency time (t_{DCP}) decreases from 130 to 33 s. Therefore, increasing the cooling rate postpones the dendrite coherency, and the dendrites become coherent later.

Keywords ADC12 aluminum alloy · Thermal analysis · Cooling rate · Dendrite coherency point (DCP) · Solidification

Introduction

The ADC12-type alloy is one of the most widely used aluminum die casting alloys and is used for many components in automotive industry [1]. In designing cast

components, it is necessary to monitor the solidification of alloys in the different cooling conditions that correspond to various cross sections of the casting as cooling rate influenced the thermo-physical properties and consequently the microstructure and mechanical properties [2]. A deeper understanding of the effect of the cooling rate on the solidification process has come to light in recent years. The effect of the cooling rate on the structural features of aluminum die casting alloys has been investigated by many authors [3–9]. According to their works, increasing the cooling rate refines all microstructural features including grain size, dendrite arm spacing (DAS) and intermetallic phases. Dendrite arm spacing is affected by increasing the cooling rate much more than other microstructural features. Variety in the cooling rate also affected many solidification characteristics such as nucleation temperature ($T_{N,a}$), nucleation undercooling ($DT_{N,a}$), growth temperature ($T_{G,a}$), solidification range (DT_s), total solidification time (t_f) and DCP [3–9].

During equiaxed dendritic solidification, the dendritic crystals are separated and can move freely in the early stage of the solidification process. With the growth of the dendrite, the dendrite tips begin to impinge upon their neighbors, such that a dendritic network is established throughout the solidifying volume. The term dendrite coherency point refers to this point or stage [10–12]. For some time, the DCP has been recognized as an important characteristic in cast aluminum alloys. It marks the transition from mass feeding to interdendritic feeding in solidification process [13]. Casting defects, such as macrosegregation, shrinkage porosity and hot tearing formed during equiaxed dendritic growth start to develop after DCP [14]. Thus, several authors have suggested that the coherency point may be an important indicator for alloy cast ability [10, 15, 16]. Therefore, a good understanding of

✉ M. Malekan
mmalekan@ut.ac.ir

¹ School of Metallurgy and Materials Engineering, College of Engineering, University of Tehran, P.O. Box 14395-515, Tehran, Iran

² Department of Mechanical Engineering, Shahid Rajaei Teacher Training University (SRTTU), Lavizan, Tehran, Iran

solidification behavior at the DCP and factors that affect the DCP is important.

The thermal analysis method uses the two-thermocouple technique developed by Bäckerud et al. [1, 17] for determining the DCP. One thermocouple is located at the center of a crucible, and the other one at the inner wall. This technique is based on the assumption that the established dendritic network at the DCP will result in a rapid decrease in the temperature difference between the wall and the central regions, due to the higher thermal conductivity of the solid material compared with the liquid. The DCP is then determined by measuring the maximum point of the temperature difference.

Much research has been focused on the effect of cooling rate on microstructural features and mechanical properties. However, change in phase nucleation temperatures, nucleation and recalescence undercooling, solidification ranges and DCP with increasing cooling rate has not been extensively investigated in the literature. In the current work, the effect of different cooling rates on the solidification parameters and dendrite coherency point of ADC12 aluminum alloy was investigated. Solidification characteristics including range and time of solidification, nucleation and recalescence undercooling, temperature and time related to the start and end of phase transformation, dendrite coherency point and fraction of solid were analyzed.

Experimental

Commercial ADC12 aluminum alloy ingots were used in this study. The chemical composition was measured by optical emission spectrometry (OES) and given in Table 1. Five hundred grams of the alloy was melted in an electrical resistant furnace in each experiment, and the melt was maintained at a temperature of 750 ± 5 °C.

After melting, the oxide layer on the surface was skimmed and the molten metal poured into the mold. Five different molds were used to obtain different cooling rates ($1.2\text{--}7.2$ °C s⁻¹) including three types of CO₂ sand molds with different wall thicknesses (10, 20 and 40 mm), one stainless steel mold with a thickness of 1 mm and one graphitic mold with a thickness of 8 mm. Dimensions of the mold with a thickness of 1 mm are schematically

shown in Fig. 1. All molds were preheated at 200 °C before pouring.

Cooling curve thermal analysis (CCTA) was performed on all samples using high sensitivity thermocouples of K type, and data were acquired by a high-speed data acquisition system (A/D converter) linked to a computer.

To record the time–temperature data, ADAM-4000 Utility software was installed on the computer. The test was conducted by embedding two thermocouples located in the middle and the wall of each mold at a position of 30 mm from the bottom of the mold (Fig. 1). In each test, data were recorded with the frequency of 20 readings per second and then transferred to origin pro9.0 software and processed. The processed included smoothing, curve fitting, plotting the first derivatives, identifying the onset and end of solidification, determining solidification parameters such as cooling rate, nucleation temperature, nucleation and recalescence undercooling, solidification range and total solidification time.

The temperature difference between the wall and the central regions ($DT = T_w - T_c$) during solidification was determined, and the DT curve was plotted in each try. The first minimum point of the DT curve (or the first maximum in temperature difference) after nucleation has been used to determine the DCP. The fraction of solid and the related

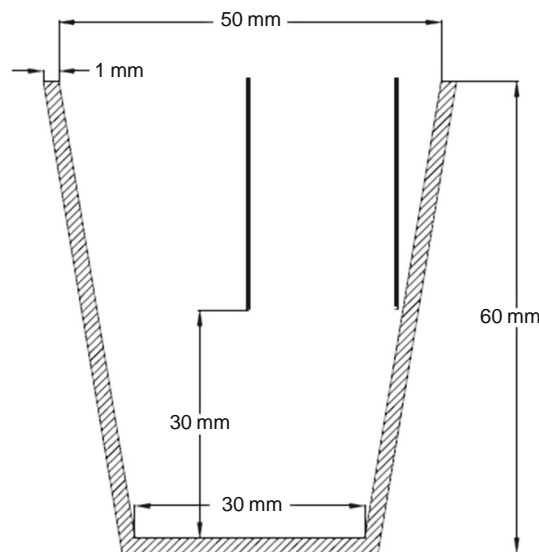
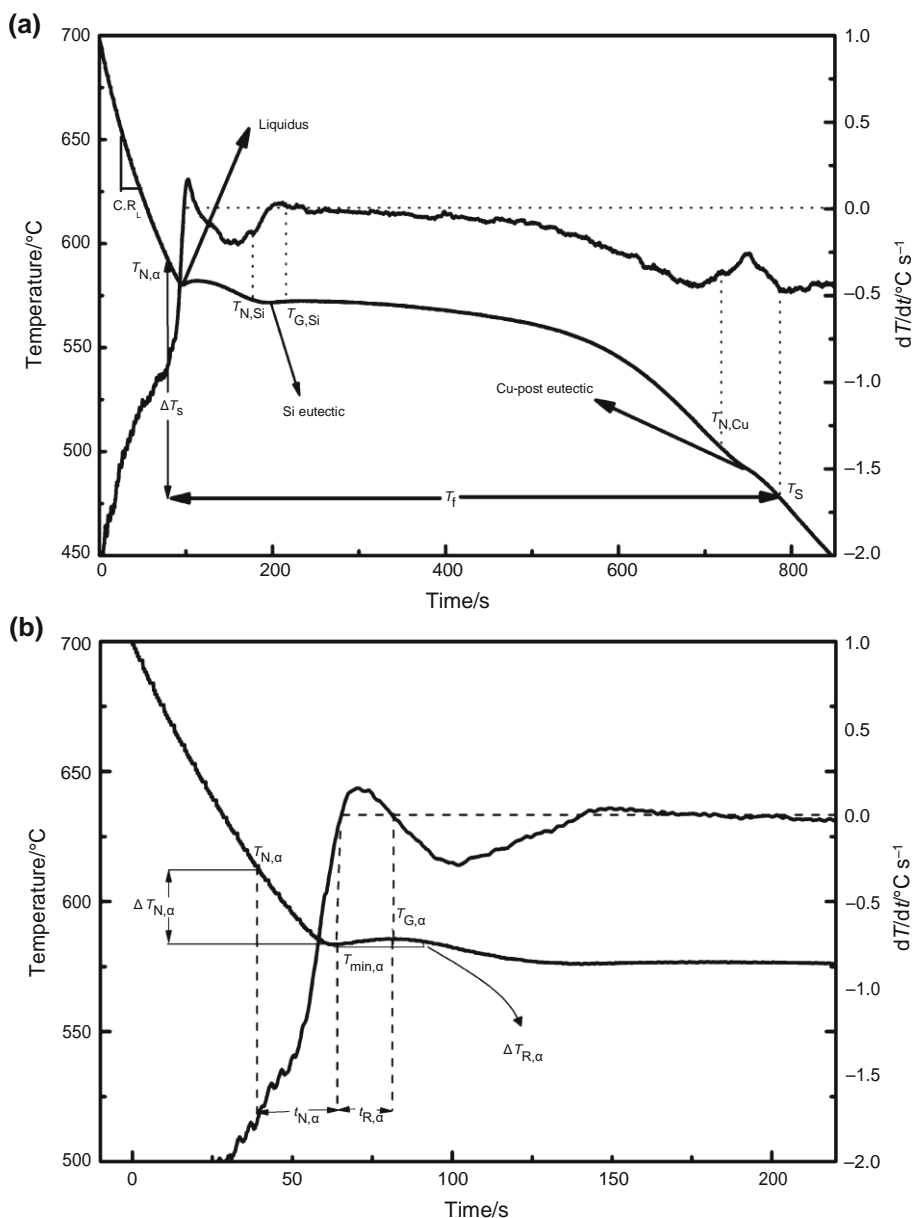


Fig. 1 Thermocouple setting in thin-wall steel mold

Table 1 Chemical composition of ADC12 aluminum die casting alloy

Alloy composition/mass%	Element					
	Si	Fe	Cu	Mn	Mg	Zn
ADC12 (standard)	9.6–12	Max 1.3	1.5–3.5	Max 0.5	Max 0.3	Max 1
ADC12 (actual sample)	9.6	0.72	2.5	0.3	0.25	1

Fig. 2 a Cooling curve, first derivative curve and representation of characteristic parameters for ADC12 alloy, b magnified liquidus region of the cooling curve and its first derivative curve for ADC12 alloy



temperature point, f_s^{DCP} and T_{DCP} , were also calculated. In this article, the thermal analysis technique has been used to quantify the fraction of solid during the solidification process of the test sample. The amount of heat evolved from a solidifying test sample can be calculated as the integrated area between the first derivative curve and the zero curve (base line). This amount of heat is proportional to the fraction of solid. Calculation accuracy depends heavily on the evaluation of the zero curve. The analysis presented in this article for zero curve calculation is based on the Newtonian model adopted by Stefanescu et al. [18, 19]. Therefore, in order to determine the fraction of solid, the cooling curve (CC), first derivative curve and zero curve (ZC) were plotted. Finally, the fraction of solid was numerically calculated from Eq. (1):

$$F_s = \frac{Cp}{L} \int_0^t \left[\left(\frac{dT}{dt} \right)_{cc} - \left(\frac{dT}{dt} \right)_{zc} \right] dt$$

$$= Cp/L (\text{area between the derived cooling curve and the zero curve at time } t) \quad (1)$$

Results and discussion

Cooling curves

Figure 2a shows the cooling curve and its first derivative of ADC12 alloy. The liquidus, Al-Si eutectic and copper

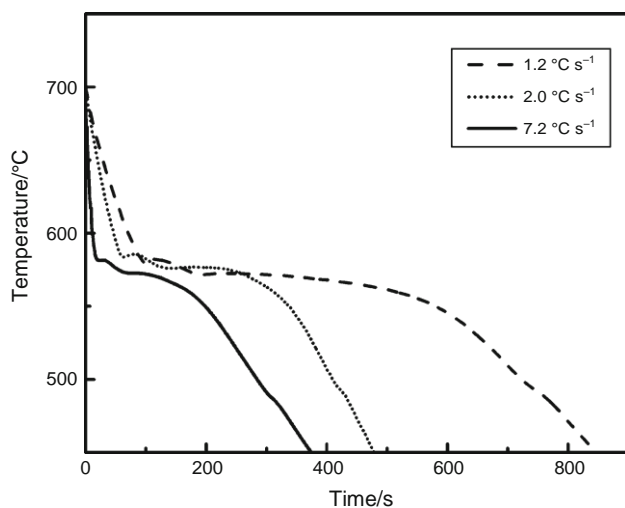


Fig. 3 Cooling curves of ADC12 alloy at various solidification conditions

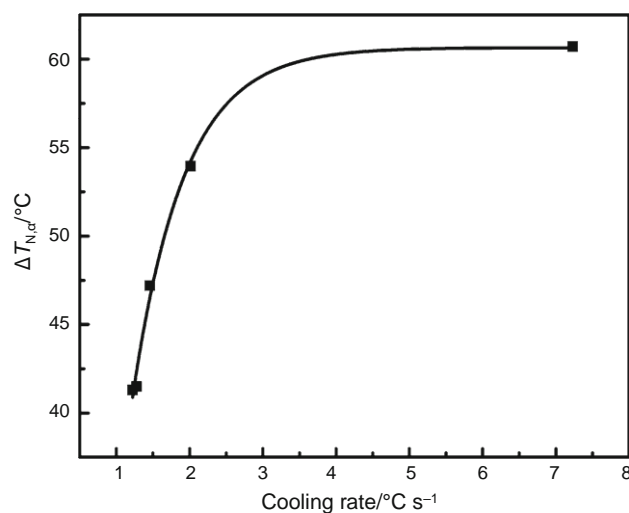


Fig. 5 Effect of the cooling rate on the nucleation undercooling temperature

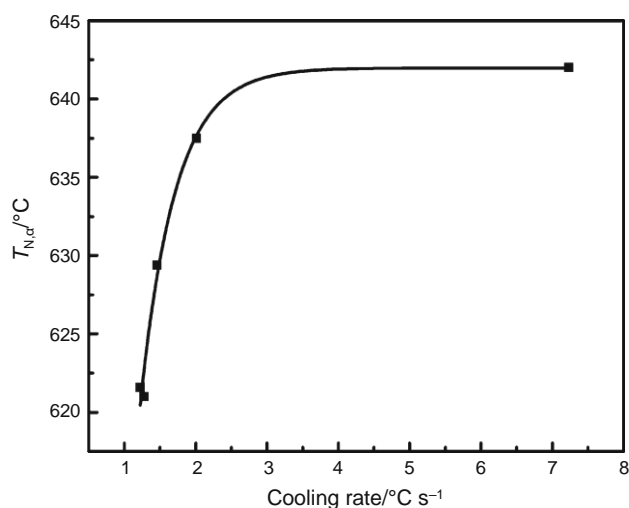


Fig. 4 Effect of the cooling rate on the nucleation temperature

posteutectic are three important regions shown on this diagram. A magnified liquidus region of the cooling curve and its first derivative curve for ADC12 alloy are shown in Fig. 2b. The most important cooling parameters are located on each region of the cooling curves. The various parameters measured from cooling and derivative curves are the liquidus parameters, solidification range, total solidification time and dendrite coherency point. To calculate the cooling rate (CR), slope of the curve at the temperature range of 590–650 °C is measured.

The cooling curves recorded for ADC12 alloy at various cooling rates are shown in Fig. 3. It is seen that the various phase regions are relocated when the cooling rate is increased. This relocation changes the characteristic parameters of thermal analysis particularly in the liquidus region. As the cooling rate is increased, the cooling curves become less sharp.

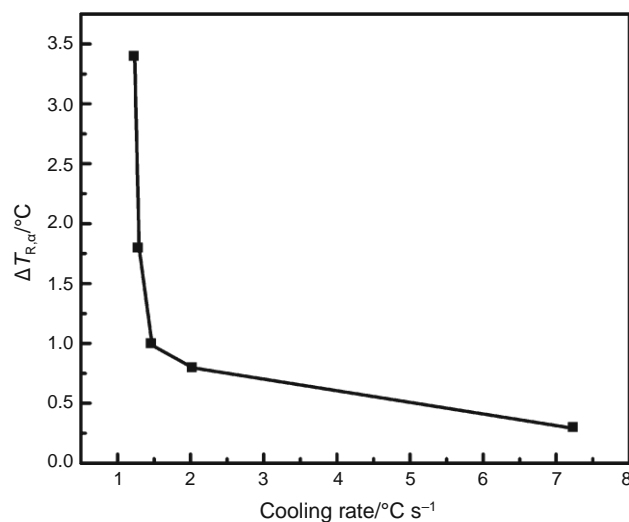


Fig. 6 Effect of the cooling rate on the recalescence undercooling temperature

The cooling rate is proportional to the heat extraction from the sample during solidification. Therefore, at a low cooling rate (1.2 °C s⁻¹), the rate of heat extraction from the sample is slow and the slope of the cooling curve is small. Therefore, it creates a wide cooling curve. But, at a high cooling rate (7.2 °C s⁻¹) the rate of heat extraction from the sample is fast, the slope of the cooling curve is steep, and it makes a narrow cooling curve.

Liquidus parameters

Figure 4 shows the effect of the cooling rate on the nucleation temperature (liquidus temperature) of ADC12 alloy. As the cooling rate increases from 1.2 to 7.2 °C s⁻¹,

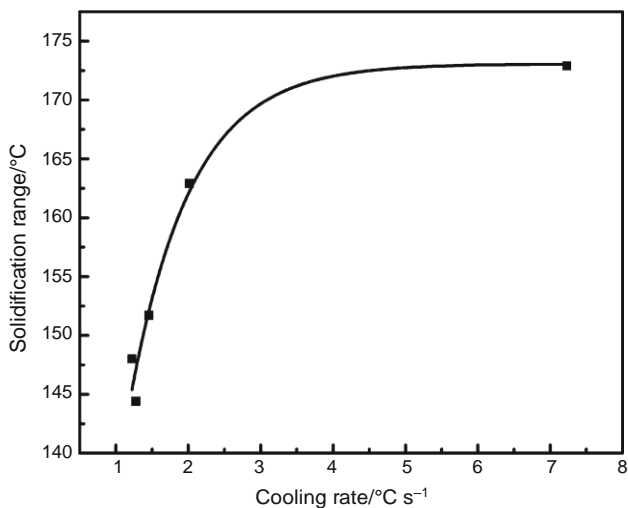


Fig. 7 Effect of the cooling rate on solidification range

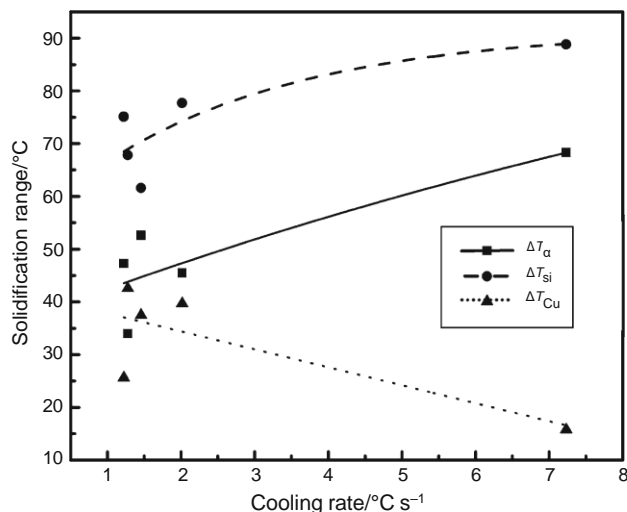


Fig. 9 Effect of the cooling rate on solidification range of various phases

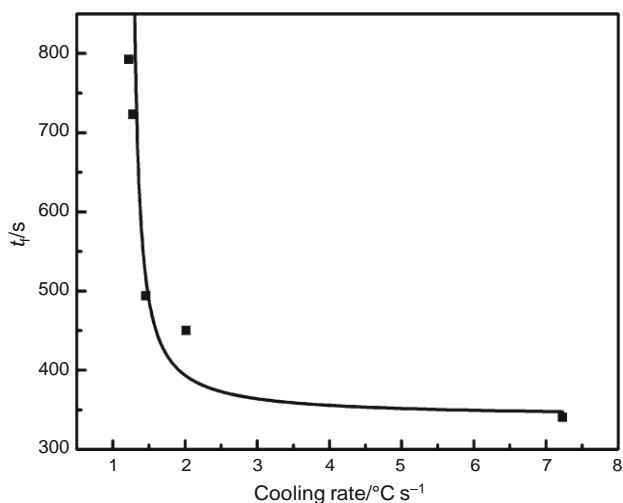


Fig. 8 Effect of the cooling rate on total solidification time

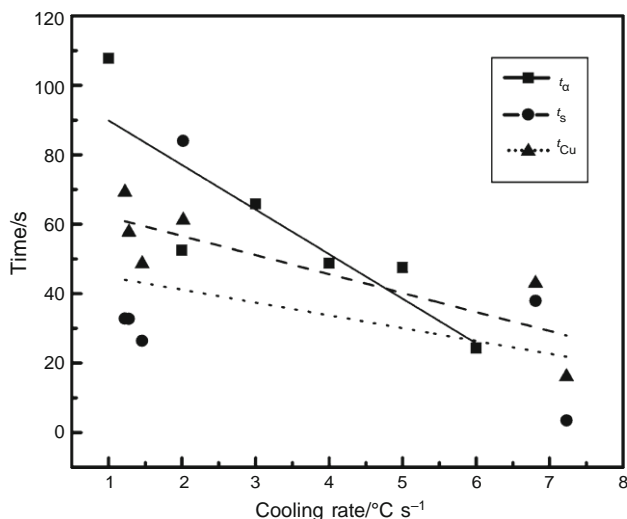


Fig. 10 Effect of the cooling rate on solidification time of various phases

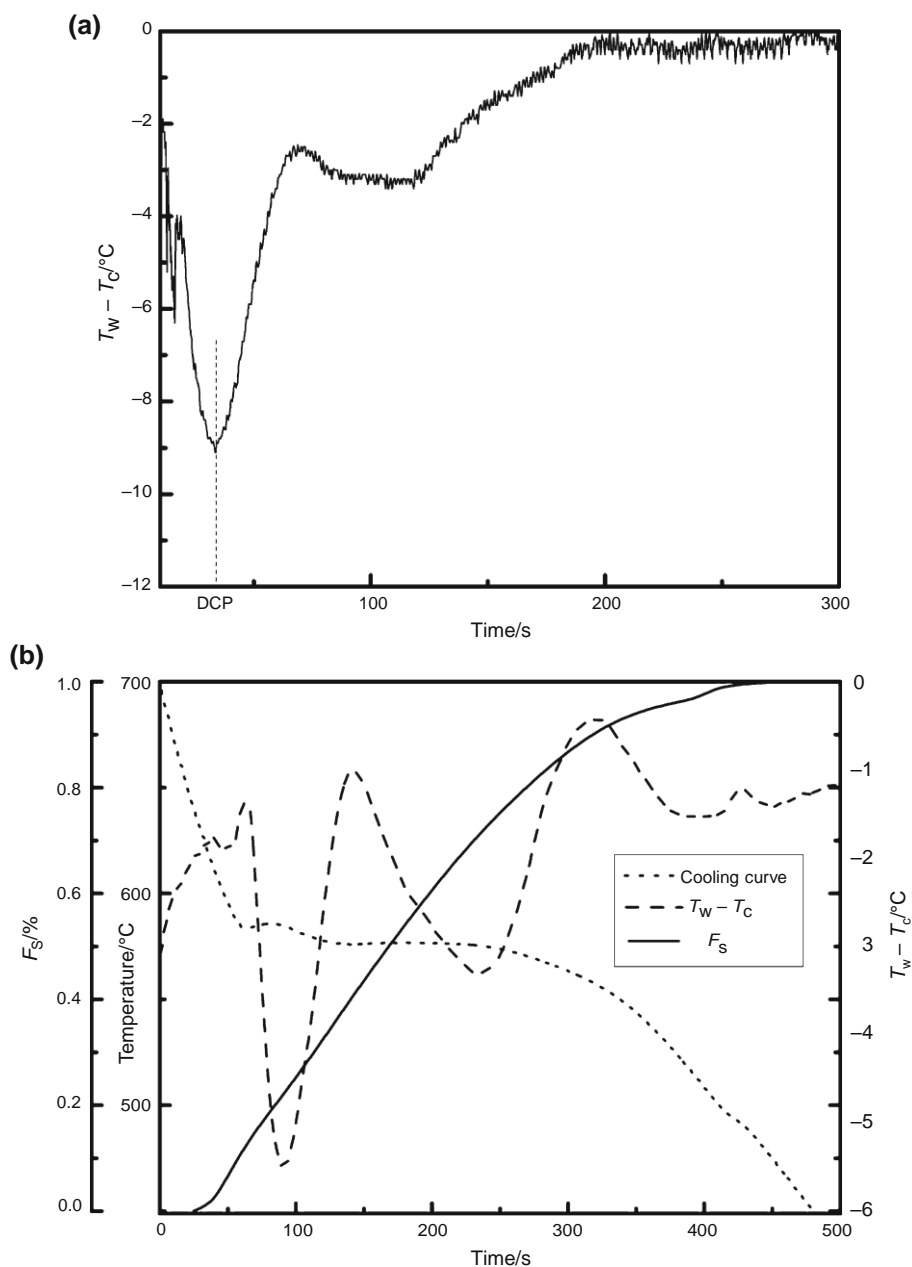
the liquidus temperature increases from 621 to 642 °C. Increasing the cooling rate increases the heat extraction. Therefore, the melt is cooled to a lower temperature than the equilibrium melting point. This situation provides more nuclei to be nucleated because of the existing appropriate undercooling. Therefore, nucleation is continued easily and quickly.

In other words, with decrease in melt temperature from equilibrium melting point, the solid phase becomes stable in terms of thermodynamics and a liquid-to-solid transition starts. The speed of this transition depends mainly on heat extraction speed. The higher cooling rate would give a faster heat extraction speed and more undercooling. It results an easier and faster nucleation which increases nucleation temperature or melting temperature. On the other hand, nucleation temperature has an

opposite relation with the energy barrier for nucleation. Thus, the increase in cooling rate decreases the energy barrier and results in the higher nucleation temperature. Shabestari and Malekan [3] have also mentioned same trend for 319 aluminum alloy.

The nucleation and recalescence undercooling temperatures, $DT_{N,a}$ and $DT_{R,a}$, measured for ADC12 alloy at various cooling rates are shown in Figs. 5 and 6. The increasing cooling rate from 1.2 to 7.2 °C s⁻¹ increases the nucleation undercooling increases about 19.4 °C and the recalescence undercooling decreases from 3.41 to 0.5 °C. A fast cooling rate causes the increase in heat extraction rate from the melt, and more existing nuclei in the melt become active. The growth condition is facilitated. On the

Fig. 11 a Plot of temperature difference between wall and center of the mold for ADC12 alloy ($7.2\text{ }^{\circ}\text{C s}^{-1}$), b the method for calculating the fraction of solid at DCP ($2\text{ }^{\circ}\text{C s}^{-1}$)



other word, with increase in cooling rate, the melt is cooled to a temperature lower than temperature of melting curve, and as a result, the undercooling of nucleation increases and this makes nucleation easier. Similar to crystalline growth, the driving force of nucleation is a function of undercooling produced during solidification process. In the event that there are enough heterogeneous nuclei, the observed undercooling hardly exceeds a few degrees but when the liquid is purified, without contacting these nuclei, undercooling plays a more important role in nucleation. This amount of undercooling can be provided by a higher cooling rate. The relation between cooling rate and the amount of undercooling can be very practical as it shows

the relation between growth condition (cooling rate) and nucleation potential (nucleation undercooling). Emadi and Whiting [20] and Backerud et al. [1] reported similar results.

Some researchers [1, 3, 8] declared that heat exchange decreases with finer structure, as in proper nucleation the need of heating eliminates. Since fast cooling results in relative nucleation, therefore decrease in recalescence undercooling is expected. Since determining of $DT_{R,a}$ on the cooling curve is easy, the relation of cooling rate and recalescence undercooling can be used to determine the ability of nucleation. These results are in approval with results reported by Anantha Narayanan et al. [21].

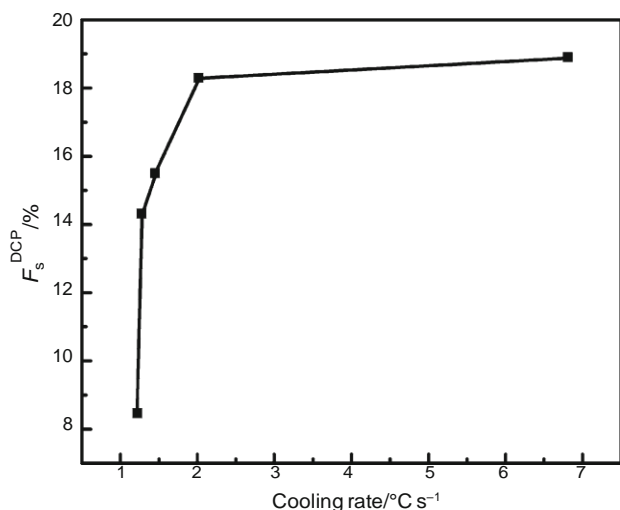


Fig. 12 Effect of cooling rate on fraction of solid at DCP for ADC12 alloy

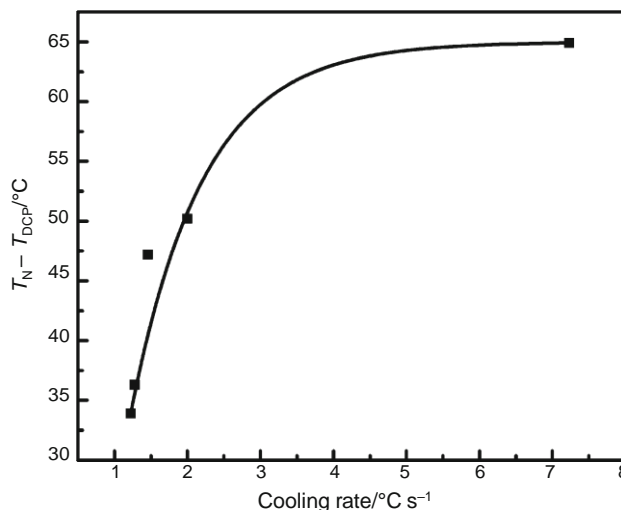


Fig. 14 Effect of cooling rate on the difference between the liquidus and coherency temperatures (T_N - T_{DCP})

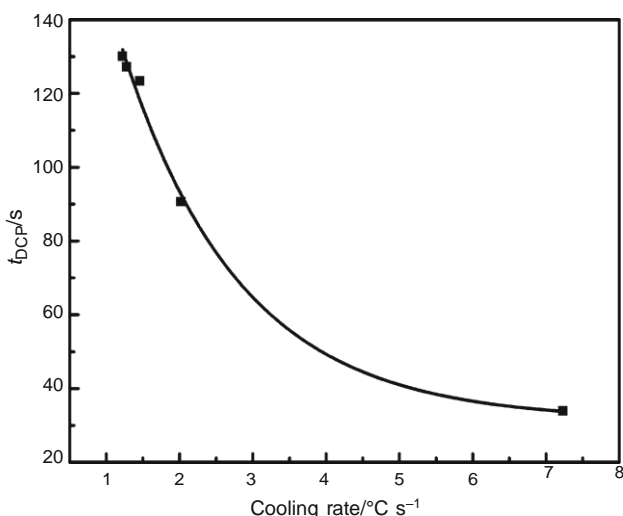


Fig. 13 Effect of cooling rate on the dendrite coherency time for ADC12 alloy

Solidification range and total solidification time

The solidification range is defined as the difference in temperatures between the first and the last liquid to solidify. Total solidification time is also the time interval between the start and the end of solidification. Figures 7 and 8 show the effect of the cooling rate on the solidification range (DT_s) and solidification time (t_f), respectively. As the cooling rate increases from 1.2 to 7.2 °C s⁻¹, the solidification range increases about 25 °C, but the total solidification time decreases about 452 s (about 7.5 min). It can also be seen in Fig. 3; with increasing the cooling rate, the cooling curve is dragged vertically and compressed horizontally. This occurrence is the result of fast

development of the solidification front and its direct relation with cooling time and wider solidification range. Solidification time is related to the cooling rate according to Eq. (2) [22]:

$$t_f \propto A \dot{C} R B^{-n} \tag{2}$$

where A and n are constants of the equation.

The solidification ranges for the formation and growth of the a-Al dendrites (DT_a = T_{N,a} - T_{N,Si}), Al-Si eutectic (DT_{Si} = T_{N,Si} - T_{N,Cu}) and Cu-rich phase (DT_{Cu} = T_{N,Cu} - T_s) have been plotted versus the cooling rate in Fig. 9. It is seen that increasing the cooling rate increases the solidification range of a-Al dendrites and Al-Si eutectic formation, but decreases DT_{Cu}. Therefore, at high cooling rates, a greater volume of a-Al dendrites and Al-Si eutectic forms. The effect of the cooling rate on the solidification time of a-Al dendrites (t_a), Al-Si eutectic (t_{si}) and Cu-rich phase (t_{cu}) is shown in Fig. 10. As seen, a decrease in total solidification time has occurred in the dendrite network growth, the Al-Si eutectic and Cu-rich phase formation and this decrease is more significant in t_a. Gowri [23] has also reported the decrease in total solidification time as a function of the cooling rate for 356 and 359 alloys. Solidification range and total solidification time are important input parameters for any solidification modeling.

Dendrite coherency point

A typical temperature difference curve between the wall and center of the mold against solidification time (DT curve) for ADC12 alloy is shown in Fig. 11. The minimum of the curve is DCP, because the progressive

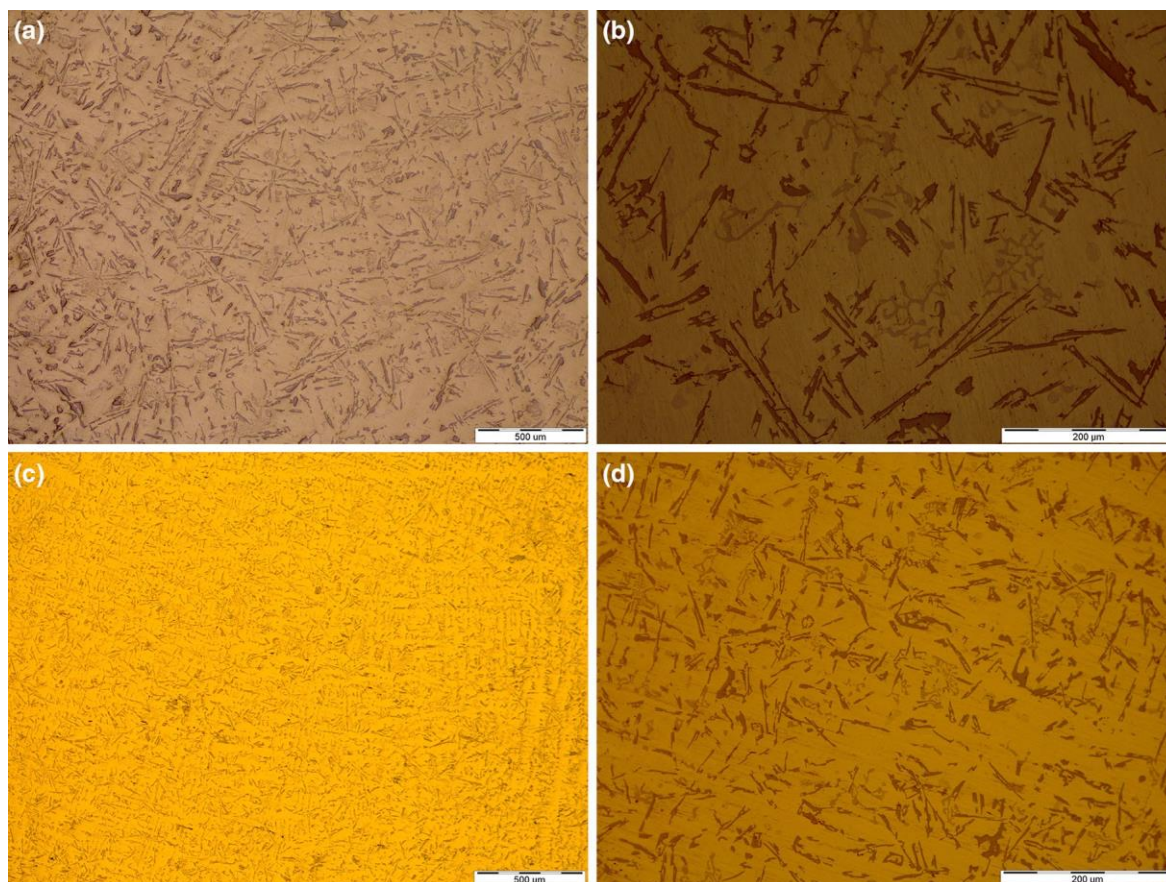


Fig. 15 Microstructure of ADC12 alloy solidified at the cooling rate of: a, b $1.2\text{ }^{\circ}\text{C s}^{-1}$, c, d $7.2\text{ }^{\circ}\text{C s}^{-1}$

growth of the dendrites stops in the center, and then, the DT curve begins to return to the steady-state value of approximately $0\text{ }^{\circ}\text{C}$ as the dendrites thicken throughout the casting.

One of the most important applications of DCP in casting is improving risering ability and decreasing porosity by increasing the fraction of solid in the coherency point. After DCP, the liquid must pass through dendritic solid frame and spacing areas. Thus, efforts to postpone DCP and increasing fraction of solid before the formation of dendritic skeleton help to prevent the formation of castings defects. Fraction of solid at DCP is so important that Campbell [24] mentioned it as risering ability and porosity formability.

Figure 12 shows the effect of cooling rate on fraction of solid at DCP for ADC12 alloy. It is seen that when cooling rate increases from 1.2 to $7.2\text{ }^{\circ}\text{C s}^{-1}$, fraction of solid at coherency point increases to about 11%. Increasing the growth rate of dendrites and finer grain size at higher cooling rates may be the reason, so dendrite arm impact occurs in finer structures and more fraction of solid.

The effect of cooling rate on the dendrite coherency time is shown in Fig. 13. As the cooling rate increases from 1.2 to $7.2\text{ }^{\circ}\text{C s}^{-1}$, the dendrite coherency time decreases

from 130 to 33 s. This is due to intensifying the nucleation rate. On the other hand, as the cooling rate is increased, all of reactions during the solidification occur in a shorter time intervals. These results are also in approval with those reported by Farahany et al. [2], Gowri and Samuel [4] and Ghoncheh and Shabestari [9]. To study the DCP, the temperature range of $T_N - T_{DCP}$ is more important than the individual temperatures of T_N or T_{DCP} . Figure 14 shows the effect of cooling rate on the temperature difference between the liquidus and coherency temperatures ($T_N - T_{DCP}$) for ADC12 alloy. When the cooling rate is increased from 1.2 to $7.2\text{ }^{\circ}\text{C s}^{-1}$, $T_N - T_{DCP}$ increases from 33.9 to $64.9\text{ }^{\circ}\text{C}$.

Microstructure

Microstructure of ADC12 alloy at two cooling rates of 1.2 and $7.2\text{ }^{\circ}\text{C s}^{-1}$ is demonstrated in Fig. 15. The microstructures of the alloy include a-Al dendrites, eutectic silicon and intermetallic phases such as Al_3FeSi (b-phase) with needle-like morphology, $\text{Al}_{15}(\text{Fe,Mn})_3\text{Si}_2$ (a-phase) with Chinese script morphology and Al_2Cu (Cu-rich phase) particles. Increasing the cooling rate refines all

microstructural features including dendrite cells, DAS, eutectic silicon and intermetallic compounds.

Conclusions

The effect of the cooling rate on solidification parameters and dendrite coherency point of ADC12 aluminum die casting alloy was studied. The results are summarized as follows:

1. Solidification parameters are affected by the cooling rate. The formation temperature of various phase are displaced with an increasing cooling rate.
2. Increasing the cooling rate significantly increases the liquidus temperature, nucleation undercooling temperature, solidification range and decreases the recalescence undercooling temperature and total solidification time.
3. Augmentation in cooling rate can increase the temperature interval of dendrite coherency ($T_N - T_{DCP}$) and coherency fraction solid (f_s^{DCP}) about 31 °C and 11 %, respectively, but the coherency time (t_{DCP}) decreases from 130 to 33 s. Therefore, increasing the cooling rate postpones the dendrite coherency, and the dendrites become coherent later.
4. Determination of DCP has many applications in casting, feeding processes and semisolid metal casting.
5. Increasing the cooling rate refines all microstructural features including dendrite cells, DAS, eutectic silicon and intermetallic compounds.

References

1. Bäckerud L, Chai G, Tamminen J. Solidification characteristics of aluminum alloys. Vol. 2. Foundry alloys. Stockholm, Sweden: AFS/Skanaluminium; 1990.
2. Farahany S, Ourdjini A, Idris MH, Shabestari SG. Investigation of the effect of solidification conditions and silicon modifier/refiner on the nucleation and growth of dendrites in near eutectic Al–Si–Cu–Fe alloy by thermal analysis. *J Therm Anal Calorim*. 2013;114:705–17.
3. Shabestari SG, Malekan M. Thermal analysis study of the effect of the cooling rate on the microstructure and solidification parameters of 319 aluminum alloy. *Can Metall Q*. 2005;44:305–12.
4. Gowri S, Samuel FH. Effect of cooling rate on the solidification behavior of Al-7 Pct Si-SiC_p metal-matrix composites. *Metall Mater Trans A*. 1992;23:3369–76.
5. Dobrzański LA, Maniara R, Sokółowski J, Kasprzak W. Effect of cooling rate on the solidification behavior of AC AlSi7Cu2 alloy. *J Mater Process Technol*. 2007;191:317–20.
6. Hosseini VA, Shabestari SG, Gholizadeh R. Study of the cooling rate on the solidification parameters, microstructure, and mechanical properties of LM13 alloy using cooling curve thermal analysis technique. *Mater Des*. 2013;50:7–14.
7. Mackay RI, Djurdjevic MB, Sokolowski JH. Effect of cooling rate on fraction solid of metallurgical reactions in 319 alloy. *AFS Trans*. 2000;108:521–30.
8. Ghoncheh MH, Shabestari SG, Abbasi MH. Effect of cooling rate on the microstructure and solidification characteristics of Al2024 alloy using computer-aided thermal analysis technique. *J Therm Anal Calorim*. 2014;117:1253–61.
9. Ghoncheh MH, Shabestari SG. Effect of Cooling Rate on the Dendrite Coherency Point during Solidification of Al2024 Alloy. *Metall Mater Trans A*. 2014;46:1287–99.
10. Malekan M, Shabestari SG. Effect of grain refinement on the dendrite coherency point during solidification of the A319 aluminum alloy. *Metall Mater Trans A*. 2009;40:3196–203.
11. Yuan L, Sullivan CO, Gourlay CM. Exploring dendrite coherency with the discrete element method. *Acta Mater*. 2012;60:1334–45.
12. Stangeland A, Mo A, Nielsen Ø, Eskin DG, Hamdi MM. Development of thermal strain in the coherent mushy zone during solidification of aluminum alloys. *Metall Mater Trans A*. 2004;35:2903–15.
13. Chavez-Zamarripa R, Ramos-Salas JA, Talamantes-Silva J, Valtierra S, Colas R. Determination of the dendrite coherency point during solidification by means of thermal diffusivity analysis. *Metall Mater Trans A*. 2007;38:1875–9.
14. Veldman NLM, Dahle AK, Stjohn DH, Arnberg L. Dendrite coherency of Al–Si–Cu alloys. *Metall Mater Trans A*. 2001;32:147–55.
15. Arnberg L, Backerud L, Chai G. Solidification characteristics of aluminum alloys. *Mater Sci Eng A*. 1993;173:101–3.
16. Jiang H, Kierkus WT, Sokolowski JH. Determining dendrite coherency point characteristics of Al alloys using single-thermocouple technique. *AFS Trans*. 1999;68:169–72.
17. Arnberg L, Backerud L, Chai G. Solidification characteristics of aluminum alloys. Vol. 3. Dendrite Coherency. Des Plaines, IL: AFS; 1996.
18. Barlow JO, Stefanescu DM. Computer-aided cooling curve analysis revisited. *AFS Trans*. 1997;105:349–54.
19. Upadhyay KG, Stefanescu DM, Lieu K, Yeager DP. *AFS Trans*. 1989;97:61–6.
20. Emadi D, Whiting LV. Determination of solidification characteristics of Al–Si alloys by thermal analysis. *AFS Trans*. 2002;110(02–033):285–96.
21. Anantha Narayanan L, Samuel FH, Gruzleski JE. Thermal analysis studies on the effect of cooling rate on the microstructure of 319 aluminum alloys. *AFS Trans*. 1992;100:383–91.
22. Kumar P, Gaiindhar JL. DAS, solidification time and mechanical properties of Al-11%Si alloys V-processed castings. *AFS Trans*. 1997;105:635–8.
23. Gowri S. Comparison of thermal analysis parameters of 356 and 359 alloys. *AFS Trans*. 1994;102:503–8.
24. Campbell J. Feeding mechanisms in castings. *AFS Cast Metals Res J*. 1969;5:1–8.